IJME

Int. J. of Applied Mechanics and Engineering, 2026, vol.???, No.???, pp.???-???
DOI: 10.59441/ijame/220171

A THREE-BRANCH VISCOELASTIC MODEL FOR ELASTIC WAVE PROPAGATION IN POROUS MEDIA WITH GAS BUBBLES

Adham A. Ali[1*] and Fatima Z. Ahmed[2]
[1]Software Department, University of Kirkuk, IRAQ
[2]Mathematics Department, University of Kirkuk, IRAQ
E-mail: adham.ali@uokirkuk.edu.iq

This research investigates the propagation of elastic waves in fluid-saturated granular media. On the linear P1-waves, complex rheology is considered, which is impacted by gas bubbles. In Biot's theory, we used stress-strain relations for the wave, which comprise three branches, including fluid continuum, solid continuum and bubbles inside the fluid. These stress-strain relations are combined with momentum, continuity and bubble dynamics equations to drive the Nikolaevskiy-type equation. In the moving reference system, the equation explains the solid matrix's velocity. Our investigation into the influence of gas bubbles on wave propagation in a fluid-saturated granular media revealed that the presence of such bubbles significantly reduces wave velocity.

Key words: porous media, bubbles, rheology, Frenkel-Biot's waves

1. Introduction

In fluid-saturated porous media, the propagation of elastic waves is of great practical and theoretical significance to engineering and science. As a two-phase system, the fluid-saturated granular medium is presented and comprises fluid and solid phases. Depending on the study conducted by Terzaghi [1, 2], a coupled deformation theory of fluid-saturated porous elastic solids was formulated by Biot [3]. Frenkel [4] simultaneously established his theory of physical processes in saturated soil.

The stress wave propagation theory's principles consisting of compressible viscous fluid are determined, such as in the studies of Biot [5, 6]. In isotropic porous media, Biot [7, 8] used the Lagrangian approach and Hamilton's principle to analyze a comprehensive system of dynamic equations governs wave propagation. According to Biot's theory, this includes two types of longitudinal (primary) waves, referred to as P-waves, and one type of transverse (secondary) wave, known as the S-wave. The P-waves are classified into two categories. While the first type has slower decay (P1-wave) and higher velocity, the latter has faster decay (P2-wave) and lower velocity. Using a synthetic rock, Plona [9] conducted the first experimental observation. In natural rocks (sandstone), this wave has been later detected, both water-saturated and air-saturated [10], at ultrasonic frequencies [11]. We refer the reader to the study [12] for further information about the proposed experimental techniques utilized in the P2-waves investigation. In generalized and complex media, such as bodies with voids, micropolar and nonlocal continua, materials subjected to magnetic, thermal, electrical, and moisture effects, as well as different boundary conditions and coupling theories, wave propagation and thermoelastic phenomena have been thoroughly investigated [13-18].

In recent decades, interest in partially saturated porous media has grown, as the presence of gas bubbles within the porous fluid significantly alters the wave propagation properties. The studies [19, 20] firstly analyzed the nonlinear wave propagation in liquid-gas bubble mixtures explaining weakly nonlinear waves. Numerous studies have demonstrated that even small amounts of gas bubbles can cause a significant decrease in wave velocity, along with a substantial increase in attenuation, due to bubble compression and associated

[*] To whom correspondence should be addressed

resonant effects [19-28]. Specifically, the impact of gas bubbles on the longitudinal waves using the simplest stress-strain relation has been studied by Dunin *et al.* [22].

To explain these phenomena, various porous rheological and elastic models have been developed. While classical Biot models successfully describe fully saturated media, they often fail to represent the complex internal oscillation mechanisms and dissipation processes associated with gas content. In this context, more advanced viscoelastic models, such as the Nikolaevsky model [29] based on internal oscillators, have been proposed to capture these effects. In its original physical form, Nikolaevsky equation explained how the complex stress-strain relations of the grains affected the displacement velocity of the solid framework in the absence of gas bubbles. However, most existing models still rely on simplified two-branch rheological schemes or only partially address the effect of gas bubbles. The equation is formulated as follows:

$$\frac{\partial v}{\partial t}+v\frac{\partial v}{\partial x}=\sum_{p=1}^{5}\varepsilon^{p-1}A_{p+1}\frac{\partial^{p+1}v}{\partial x^{p+1}}, \tag{1.1}$$

where solid matrix velocity is defined by v, A_{p+1} denotes the coefficients linked to the system's mechanical parameters, ε refers to a small parameter that reflects the slow evolution of the wave. The impact of dispersion, dissipation of energy, and nonlinearity can be accounted for by the terms in Eq.(1.1). Aiming to include Nikolaevskiy bubbles, Strunin [30] identified the location in the rheological scheme, where bubble-linked element must occupy (Fig.1).

In [31], gas bubbles were incorporated into a two-branch rheological scheme based on the Nikolaevskiy model presented in [32]. Subsequently, the type Eq.(1.1) was derived and analyzed. The aim of the current study is to extend this approach by considering two objectives. First, the Nikolaevsky viscoelastic model [29] is modified to include gas bubbles within a three-branch rheological scheme. Second, we analyze and derive the type (1.1) equation, in which the coefficients A_p may be influenced by parameters associated with the bubbles. Consequently, complicated constitutive law will be given by this scheme. Therefore, the main interest of the current work is to investigate the law's impact on the decay of waves.

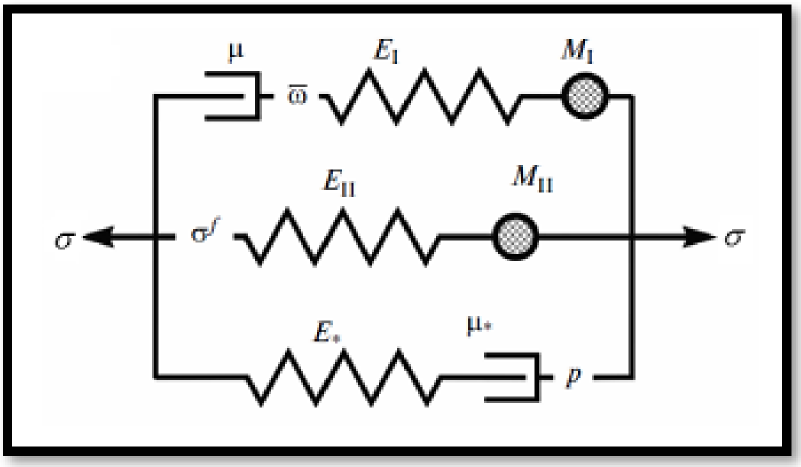

Fig.1. Rheological scheme with the branch ϖcorresponding to a bubble [30].

The rest of this article is organized as follows. Section 2 presents the mathematical model, including the equation of dynamics, dynamics of bubbles, density relations, and proposed rheological model. In Section 3, a Nikolaevskiy-type equation is derived. Section 4 explores results and discussion, incorporating the influence of gas bubble on wave velocity, sensitivity analysis, comparison with existing models, as well as computational aspects and practical relevance. Finally, Section 5 concludes this work.

2. Mathematical model overview

2.1. The equations of dynamics

A one-dimensional model is considered to describe wave propagation in a fluid-saturated porous medium containing gas bubble. Following the classical formulation for porous continua, the governing equations consist of momentum balance and mass conservation for both the solid matrix and the pore fluid. According to Nikolaevskiy [33], these equations can be written as

$$\frac{\partial}{\partial t}(1-\phi)\rho^{(s)}v+\frac{\partial}{\partial x}(1-\phi)\rho^{(s)}vv=\frac{\partial}{\partial x}\sigma^{(ef)}-(1-\phi)\frac{\partial p}{\partial x}-I\ ,$$

$$\frac{\partial}{\partial t}\phi\rho^{(f)}u+\frac{\partial}{\partial x}\phi\rho^{(f)}uu=-\phi\frac{\partial p}{\partial x}+I\ ,$$

$$\frac{\partial}{\partial t}(1-\phi)\rho^{(s)}+\frac{\partial}{\partial x}(1-\phi)\rho^{(s)}v=0\ , \tag{2.1}$$

$$\frac{\partial}{\partial t}\phi\rho^{(f)}+\frac{\partial}{\partial x}\phi\rho^{(f)}u=0\ .$$

Where the subscript sf labels the solid and (gas-liquid mixture) respectively, the corresponding densities and mass velocities are denoted by ρ, v, and u. The pore pressure is defined by p, $\sigma^{(ef)}$ refers to the effective Terzaghi stress, and the porosity is denoted by ϕ. The interfacial viscous force is defined by I, which is approximated as follows:

$$I=\delta\phi(v-u),\quad \delta=\frac{\mu^{(f)}\phi}{k}\ ,$$

where the intrinsic permeability is denoted by k and $\mu^{(f)}$ refers to the gas-liquid mixture viscosity.

2.2. Bubble dynamics

The dynamics of gas bubbles embedded in the pore fluid are described using a modified Rayleigh–Plesset-type equation, following the formulation proposed in [22, 23]. The evolution of the bubble radius is governed by:

$$R\frac{\partial^2}{\partial t^2}R+\frac{3}{2}\left(\frac{\partial}{\partial t}R\right)^2+\frac{4\mu}{\rho^{(L)}}\left(\frac{1}{R}+\frac{\phi}{4k}R\right)\frac{\partial}{\partial t}R=\left(p_g-p\right)/\rho^{(L)}\ , \tag{2.2}$$

where p refers to the pressure in the liquid, and the instantaneous bubble's radius is defined by R. Inside the bubble, the gas pressure is defined as $p_g=p_0(R_0/R)^{\chi}$, where $\chi=3\varsigma$, ς refers to the adiabatic exponent. The gas pressure inside the bubble is assumed to obey a polytropic law, μ is the liquid viscosity and $\rho^{(L)}$ is the density liquid without the bubbles.

2.3. Density relations

For the solid and the pore liquid in the absence of gas, the density variations are assumed to follow linear compressibility relations:

$$\rho^{(s)} = \rho_0^{(s)}\left(1-\beta^{(s)}\sigma\right) = \rho_0^{(s)}\left[1+\beta^{(s)}p-\frac{\beta^{(s)}\sigma^{(ef)}}{1-\phi}\right] \approx \rho_0^{(s)}\left[1+\beta^{(s)}p-\beta^{(s)}\sigma^{(ef)}\right], \tag{2.3}$$

$$\rho^{(L)} = \rho_0^{(L)}\left(1+\beta^{(L)}p\right). \tag{2.4}$$

These relations follow directly from linear elasticity theory and standard compressibility assumptions, as discussed in [23, 33]. Now, we write the mean density of the gas-liquid mixture as:

$$\rho^{(f)} = (1-V)\rho^{(L)} + V\rho^{(g)}, \tag{2.5}$$

where: $V = (4\pi/3)R^3 n_0$.

n_0 refers to the number density of the bubbles per unit volume (V), and σ refers to the true stress. Because of the low gas content, the density of the gas $\rho^{(g)}$ can be neglected. Because of the change in the bubble radius R , the volume (V) is changed.

Accordingly, Eq.(2.5) can be written as follows:

$$\rho^{(f)} = \rho_0^{(L)}\left(1+\beta^{(L)}p\right)\left(1-\frac{4\pi}{3}R_0^3 n_0\right). \tag{2.6}$$

The pore pressure p assumed to be equal to the pressure in the liquid far from the bubble (similarly to [23]).

2.4. Proposed rheological model

In this section, we derive the stress–strain relationship for a viscoelastic medium using the Maxwell-Voigt rheological model, which accounts for the presence of gas bubbles. The model is composed of the following elements:

A. 2 friction elements with viscosities μ_1 and μ_2.

B. 3 oscillating masses M_1, M_2 and M_3.

C. 4 elastic springs with the elastic moduli E_1, E_2, E_3 and E_4.

Hence, σ denotes the toral stress, and e refers to the displacements of the model elements with respective subscripts (Fig.2). By applying Newton's second law to each oscillating element and combining the corresponding kinematic relations, a system of coupled differential equations is obtained as follows:

$$\begin{gathered} M_1\frac{d^2e_1}{dt^2} + M_2\frac{d^2e_2}{dt^2} = \sigma - E_1e_1 - E_2e_2 - E_4e_5 \ , \\ e = e_2 = e_5 + e_6 = e_1 + e_3 + e_4 \ , \end{gathered} \tag{2.7}$$

$$M_3 \frac{d^2 e_3}{dt^2} = E_1 e_1 - E_3 e_3 \ ,$$

$$E_4 e_5 = \mu_2 \left(\frac{de}{dt} - \frac{de_5}{dt} \right), \tag{2.7 cont.}$$

$$E_3 e_3 = \mu_1 \frac{de_4}{dt} \ .$$

If we compare this system with our previous study [31], we find that this system is more complex. Below is the used approach to determine the constitutive law. Differentiating this system (2.7) up to the 6^{th} order with respect to time allows it to be written in compact matrix form as

$$AX = B, \tag{2.8}$$

where:

$$A = \begin{pmatrix}
E_2 & E_1 & 0 & 0 & E_4 & 0 & 0 & 0 & 0 & 0 & 0 & 0 & 0 & 0 & 0 & 0 & 0 & 0 & 0 & 0 & 0 & 0 & 0 & 0 & 0 & 0 & 0 & 0 & 0 \\
0 & 0 & 0 & 0 & 0 & E_1 & 0 & 0 & E_4 & 0 & 0 & 0 & 0 & 0 & 0 & 0 & 0 & 0 & 0 & 0 & 0 & 0 & 0 & 0 & 0 & 0 & 0 & 0 & 0 \\
0 & 0 & 0 & 0 & 0 & 0 & 0 & 0 & 0 & E_1 & 0 & 0 & E_4 & 0 & 0 & 0 & 0 & 0 & 0 & 0 & 0 & 0 & 0 & 0 & 0 & 0 & 0 & 0 & 0 \\
0 & 0 & 0 & 0 & 0 & 0 & 0 & 0 & 0 & 0 & 0 & 0 & 0 & E_1 & 0 & 0 & E_4 & 0 & 0 & 0 & 0 & 0 & 0 & 0 & 0 & 0 & 0 & 0 & 0 \\
0 & 0 & 0 & 0 & 0 & 0 & 0 & 0 & 0 & 0 & 0 & 0 & 0 & 0 & 0 & 0 & 0 & E_1 & 0 & 0 & E_4 & 0 & 0 & 0 & 0 & 0 & 0 & 0 & 0 \\
-1 & 1 & 1 & 1 & 0 & 0 & 0 & 0 & 0 & 0 & 0 & 0 & 0 & 0 & 0 & 0 & 0 & 0 & 0 & 0 & 0 & 0 & 0 & 0 & 0 & 0 & 0 & 0 & 0 \\
0 & 0 & 0 & 0 & 0 & 1 & 1 & 1 & 0 & 0 & 0 & 0 & 0 & 0 & 0 & 0 & 0 & 0 & 0 & 0 & 0 & 0 & 0 & 0 & 0 & 0 & 0 & 0 & 0 \\
0 & 0 & 0 & 0 & 0 & 0 & 0 & 0 & 0 & 1 & 1 & 1 & 0 & 0 & 0 & 0 & 0 & 0 & 0 & 0 & 0 & 0 & 0 & 0 & 0 & 0 & 0 & 0 & 0 \\
0 & 0 & 0 & 0 & 0 & 0 & 0 & 0 & 0 & 0 & 0 & 0 & 0 & 1 & 1 & 1 & 0 & 0 & 0 & 0 & 0 & 0 & 0 & 0 & 0 & 0 & 0 & 0 & 0 \\
0 & 0 & 0 & 0 & 0 & 0 & 0 & 0 & 0 & 0 & 0 & 0 & 0 & 0 & 0 & 0 & 0 & 1 & 1 & 1 & 0 & 0 & 0 & 0 & 0 & 0 & 0 & 0 & 0 \\
0 & 0 & 0 & 0 & 0 & 0 & 0 & 0 & 0 & 0 & 0 & 0 & 0 & 0 & 0 & 0 & 0 & 0 & 0 & 0 & 0 & 1 & 1 & 1 & 0 & 0 & 0 & 0 & 0 \\
0 & 0 & 0 & 0 & 0 & 0 & 0 & 0 & 0 & 0 & M_3 & 0 & 0 & 0 & 0 & 0 & 0 & 0 & 0 & 0 & 0 & 0 & 0 & 0 & 0 & 1 & 1 & 1 & 0 \\
0 & -E_1 & E_3 & 0 & 0 & 0 & 0 & 0 & 0 & 0 & 0 & 0 & 0 & 0 & 0 & 0 & 0 & 0 & 0 & 0 & 0 & 0 & 0 & 0 & 0 & 0 & 0 & 0 & 0 \\
0 & 0 & 0 & 0 & 0 & -E_1 & E_3 & 0 & 0 & -E_1 & E_3 & 0 & 0 & 0 & M_3 & 0 & 0 & 0 & 0 & 0 & 0 & 0 & 0 & 0 & 0 & 0 & 0 & 0 & 0 \\
0 & 0 & 0 & 0 & 0 & 0 & 0 & 0 & 0 & 0 & 0 & 0 & 0 & 0 & 0 & 0 & 0 & 0 & M_3 & 0 & 0 & 0 & 0 & 0 & 0 & 0 & 0 & 0 & 0 \\
0 & 0 & 0 & 0 & 0 & 0 & 0 & 0 & 0 & 0 & 0 & 0 & 0 & -E_1 & E_3 & 0 & 0 & 0 & 0 & 0 & 0 & 0 & M_2 & 0 & 0 & 0 & 0 & 0 & 0 \\
0 & 0 & 0 & 0 & 0 & 0 & 0 & 0 & 0 & 0 & 0 & 0 & 0 & 0 & 0 & 0 & 0 & -E_1 & E_3 & 0 & 0 & 0 & 0 & 0 & 0 & 0 & M_3 & 0 & 0 \\
0 & 0 & E_3 & 0 & 0 & 0 & 0 & -\mu_1 & 0 & 0 & 0 & -\mu_1 & 0 & 0 & 0 & 0 & 0 & 0 & 0 & 0 & 0 & 0 & 0 & 0 & 0 & 0 & 0 & 0 & 0 \\
0 & 0 & 0 & 0 & 0 & 0 & E_3 & 0 & 0 & 0 & E_3 & 0 & 0 & 0 & 0 & 0 & 0 & 0 & 0 & 0 & 0 & 0 & 0 & 0 & 0 & 0 & 0 & 0 & 0 \\
0 & 0 & 0 & 0 & 0 & 0 & 0 & 0 & 0 & 0 & 0 & 0 & 0 & 0 & 0 & -\mu_1 & 0 & 0 & 0 & 0 & 0 & 0 & 0 & 0 & 0 & 0 & 0 & 0 & 0 \\
0 & 0 & 0 & 0 & 0 & 0 & 0 & 0 & 0 & 0 & 0 & 0 & 0 & 0 & E_3 & 0 & 0 & 0 & 0 & -\mu_1 & 0 & 0 & 0 & 0 & 0 & 0 & 0 & 0 & 0 \\
0 & 0 & 0 & 0 & 0 & 0 & 0 & 0 & 0 & 0 & 0 & 0 & 0 & 0 & 0 & 0 & 0 & 0 & E_3 & 0 & 0 & 0 & 0 & -\mu_1 & 0 & 0 & 0 & 0 & 0 \\
0 & 0 & 0 & 0 & 0 & 0 & 0 & 0 & 0 & 0 & 0 & 0 & 0 & 0 & 0 & 0 & 0 & 0 & 0 & 0 & 0 & 0 & E_3 & 0 & 0 & 0 & 0 & -\mu_1 & 0 \\
0 & 0 & 0 & 0 & E_4 & 0 & 0 & 0 & \mu_2 & 0 & 0 & 0 & 0 & 0 & 0 & 0 & 0 & 0 & 0 & 0 & 0 & 0 & 0 & 0 & 0 & 0 & 0 & 0 & 0 \\
0 & 0 & 0 & 0 & 0 & 0 & 0 & 0 & E_4 & 0 & 0 & 0 & \mu_2 & 0 & 0 & 0 & 0 & 0 & 0 & 0 & 0 & 0 & 0 & 0 & 0 & 0 & 0 & 0 & 0 \\
0 & 0 & 0 & 0 & 0 & 0 & 0 & 0 & 0 & 0 & 0 & 0 & E_4 & 0 & 0 & 0 & \mu_2 & 0 & 0 & 0 & 0 & 0 & 0 & 0 & 0 & 0 & 0 & 0 & 0 \\
0 & 0 & 0 & 0 & 0 & 0 & 0 & 0 & 0 & 0 & 0 & 0 & 0 & 0 & 0 & 0 & E_4 & 0 & 0 & 0 & \mu_2 & 0 & 0 & 0 & 0 & 0 & 0 & 0 & 0 \\
0 & 0 & 0 & 0 & 0 & 0 & 0 & 0 & 0 & 0 & 0 & 0 & 0 & 0 & 0 & 0 & 0 & 0 & 0 & 0 & E_4 & 0 & 0 & 0 & \mu_2 & 0 & 0 & 0 & 0 \\
0 & 0 & 0 & 0 & 0 & 0 & 0 & 0 & 0 & 0 & 0 & 0 & 0 & 0 & 0 & 0 & 0 & 0 & 0 & 0 & 0 & 0 & 0 & 0 & E_4 & 0 & 0 & 0 & \mu_2
\end{pmatrix},$$

$$X=\begin{pmatrix} e\\ e_1\\ e_3\\ e_4\\ e_5\\ \dot{e}_1\\ \dot{e}_3\\ \dot{e}_4\\ \dot{e}_5\\ \ddot{e}_1\\ \ddot{e}_3\\ \ddot{e}_4\\ \ddot{e}_5\\ \dddot{e}_1\\ \dddot{e}_3\\ \dddot{e}_4\\ \dddot{e}_5\\ e_1^{iv}\\ e_3^{iv}\\ e_4^{iv}\\ e_5^{iv}\\ e_1^{v}\\ e_3^{v}\\ e_4^{v}\\ e_5^{v}\\ e_1^{vi}\\ e_3^{vi}\\ e_4^{vi}\\ e_5^{vi} \end{pmatrix},\quad B=\begin{pmatrix} \sigma-M_2\ddot{e}\\ \dot{\sigma}-E_2\dot{e}-M_2\dddot{e}\\ \ddot{\sigma}-E_2\ddot{e}-M_2e^{iv}\\ \dddot{\sigma}-E_2\dddot{e}-M_2e^{v}\\ \sigma^{iv}-E_2e^{iv}-M_2e^{iv}\\ 0\\ \dot{e}\\ \ddot{e}\\ \dddot{e}\\ e^{iv}\\ e^{v}\\ e^{vi}\\ 0\\ 0\\ 0\\ 0\\ 0\\ 0\\ 0\\ 0\\ 0\\ 0\\ 0\\ \mu_2\dot{e}\\ \mu_2\ddot{e}\\ \mu_2\dddot{e}\\ \mu_2e^{iv}\\ \mu_2e^{v}\\ \mu_2e^{vi} \end{pmatrix}.$$

The matrix A collects the coefficients associated with elastic moduli, viscosities, and oscillator masses, while the vector X contains the time derivatives of the internal displacements. The explicit structure of A follows directly from the rheological scheme shown in Fig.2 and is obtained by systematic differentiation and elimination of internal variables. Solving the matrix system yields the internal displacements in terms of the total strain. Substituting these results back into the stress balance equation leads to the constitutive relation. To obtain the value of e from System (2.8), we use the Maxima computer algebra system.

$$\begin{aligned} e={}&\frac{\sigma-\mu_1\dfrac{de}{dt}}{E_2}+\frac{\left(\left(E_1+E_3\right)E_4\mu_1-E_1E_3\mu_2\right)\dfrac{d\sigma}{dt}+\left(E_1+E_3\right)\mu_1\mu_2\dfrac{d^2\sigma}{dt^2}}{E_1E_2E_3E_4}+\\ &+\frac{M_3\mu_1\left(E_4\dfrac{d^3\sigma}{dt^3}+\mu_2\dfrac{d^4\sigma}{dt^4}\right)-\mu_1\mu_2E_1E_3\dfrac{d^2e}{dt^2}}{E_1E_2E_3E_4}+\\ &-\frac{\left(E_3M_1+E_1M_3\right)\mu_1\left(E_4\dfrac{d^3e}{dt^3}+\mu_2\dfrac{d^4e}{dt^4}\right)-M_1M_3\left(E_4\dfrac{d^5e}{dt^5}+\mu_1\mu_2\dfrac{d^6e}{dt^6}\right)}{E_1E_2E_3E_4}. \end{aligned} \tag{2.9}$$

The detailed algebraic steps leading to Eq.(2.9) have been omitted for brevity but follow standard elimination procedures for linear systems with constant coefficients [34]. Eq.(2.9) leads to the stress-strain equation:

$$\begin{gathered}\sigma+\left(\frac{\left(E_1+E_3\right)E_4\mu_1+E_1E_3\mu_2}{E_1E_3E_4}\right)\frac{d\sigma}{dt}+\left(\frac{E_1+E_3}{E_1E_3}\right)\theta_1\frac{d^2\sigma}{dt^2}+\mu_1\theta_2\frac{d^3\sigma}{dt^3}+\theta_1\theta_2\frac{d^4\sigma}{dt^4}= \\ =E_2e+\mu_1\frac{de}{dt}+\theta_1\frac{d^2e}{dt^2}+\mu_1\theta_3\frac{d^3e}{dt^3}+\theta_1\theta_3\frac{d^4e}{dt^4}+M_1\mu_1\theta_2\frac{d^5e}{dt^5}+M_1\theta_1\theta_2\frac{d^6e}{dt^6}\ ,\end{gathered} \tag{2.10}$$

where: $\theta_1=\frac{\mu_1\mu_2}{E_4},\quad \theta_2=\frac{M_3}{E_1E_3},\quad \theta_3=\frac{E_3M_1+E_1M_3}{E_1E_3}$.

Although the coefficients appearing in Eq.(2.10) have a complex algebraic structure, they represent physically meaningful combinations of elastic moduli, viscosities, and oscillator masses. To improve readability, these coefficients are grouped according to their physical origin, and their dependence on bubble-related parameters is explicitly discussed. Generalizing Eq.(2.10) using a similar approach to [34], we get:

$$\sigma^{(ef)}+\sum_{q=1}^{4}b_q\frac{D^q\sigma^{(ef)}}{Dt^q}=E_2e+\beta^{(s)}k_b\,p+\sum_{q=1}^{6}a_q\frac{D^qe}{Dt^q}\ , \tag{2.11}$$

where effective stress is denoted by $\sigma^{(ef)}$, and k_b refers to the bulk elastic module of the porous matrix. Accordingly, a_q and b_q can be written as follows:

$$a_1=\mu_1,\quad a_2=\theta_1,\quad a_3=\mu_1\theta_3,\quad a_4=\theta_1\theta_3,\quad a_5=M_1\mu_1\theta_2,\quad a_6=M_1\theta_1\theta_2,$$

$$b_1=\left(\frac{\left(E_1+E_3\right)E_4\mu_1+E_1E_3\mu_2}{E_1E_3E_4}\right),\quad b_2=\left(\frac{E_1+E_3}{E_1E_3}\right)\theta_1,\quad b_3=\mu_1\theta_2,\quad b_4=\theta_1\theta_2.$$

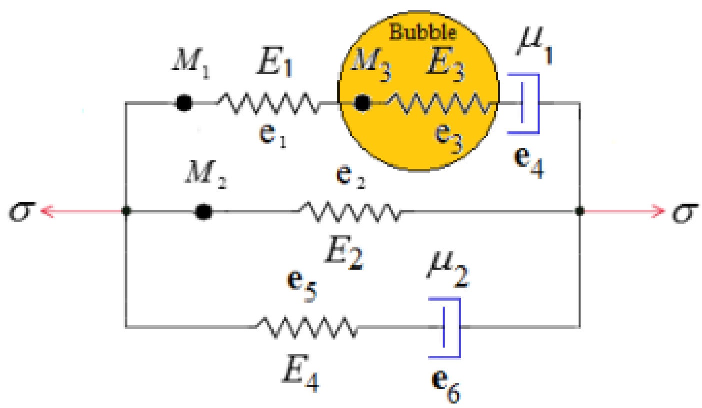

Fig.2. Three–branch rheological scheme including a gas bubble.

We add the relation between the velocity v and the matrix deformation e to complete the above set of equations:

$$\frac{De}{Dt} \equiv \frac{\partial e}{\partial t} + v\frac{\partial e}{\partial x} = \frac{\partial v}{\partial x} . \tag{2.12}$$

3. P1-wave propagation in saturated media with gas bubbles

This study examines the propagation of P1-waves within a porous medium that is entirely saturated with a compressible liquid or gas, including the presence of gas bubbles. Under this assumption, the mass velocities u and v are considered to be aligned, indicating that they share the same direction of motion:

$$v = u + O(\varepsilon v), \tag{3.1}$$

where ε refers to the small parameter. The order of the Darcy force is as follows:

$$I = \varepsilon^{\gamma}\delta\phi(v-u) = \varepsilon^{\gamma}\delta\phi v, \quad \delta = \frac{\phi\mu}{k} = O(1). \tag{3.2}$$

The running coordinate system with simultaneous scale change is used to show a weakly nonlinear wave (by following the Nikolaevskiy approach in [34]):

$$\xi = \varepsilon^{\alpha}(x-ct), \quad \tau = \frac{1}{2}\varepsilon^{\beta} t, \quad \frac{\partial}{\partial x} = \varepsilon^{\alpha}\frac{\partial}{\partial \xi}, \quad \frac{\partial}{\partial t} = \varepsilon^{\alpha}\left(\frac{1}{2}\varepsilon^{\beta-\alpha}\frac{\partial}{\partial \tau} - c\frac{\partial}{\partial \xi}\right). \tag{3.3}$$

Therefore, the following results can be obtained using the system (2.8), the constitutive law (2.11), and Eqs.(2.12) and (3.3).

$$\varepsilon^{\beta-\alpha}\frac{1}{2}\frac{\partial(1-\phi)\rho^{(s)}v}{\partial \tau} + \frac{\partial}{\partial \xi}(1-\phi)\rho^{(s)}v(v-c) = \frac{\partial \sigma^{(ef)}}{\partial \xi} - (1-\phi)\frac{\partial p}{\partial \xi} - \varepsilon^{\gamma-\alpha}\delta\phi v,$$

$$\varepsilon^{\beta-\alpha}\frac{1}{2}\frac{\partial \phi\rho^{(f)}u}{\partial \tau} + \frac{\partial}{\partial \xi}\phi\rho^{(f)}u(u-c) = -\phi\frac{\partial p}{\partial \xi} + \varepsilon^{\gamma-\alpha}\delta\phi v,$$

$$\varepsilon^{\beta-\alpha}\frac{1}{2}\frac{\partial(1-\phi)\rho^{(s)}}{\partial \tau} + \frac{\partial}{\partial \xi}(1-\phi)\rho^{(s)}(v-c) = 0,$$

$$\varepsilon^{\beta-\alpha}\frac{1}{2}\frac{\partial \phi\rho^{(f)}}{\partial \tau} + \frac{\partial}{\partial \xi}\phi\rho^{(f)}(u-c) = 0. \tag{3.4}$$

$$\begin{aligned} &\sigma^{(ef)} + \sum_{q=1}^{4} b_q\,\varepsilon^{q\alpha}\left(\frac{1}{2}\varepsilon^{\beta-\alpha}\frac{\partial}{\partial \tau} + (v-c)\frac{\partial}{\partial \xi}\right)^{q}\sigma^{(ef)} = \\ &= E_2 e + \beta^{(s)}k_b\,p + \sum_{q=1}^{6} a_q\,\varepsilon^{q\alpha}\left(\frac{1}{2}\varepsilon^{\beta-\alpha}\frac{\partial}{\partial \tau} + (v-c)\frac{\partial}{\partial \xi}\right)^{q} e, \end{aligned} \tag{3.5}$$

$$\varepsilon^{\beta-\alpha}\frac{1}{2}\frac{\partial e}{\partial\tau}+\left(v-c\right)\frac{\partial e}{\partial\xi}=\frac{\partial v}{\partial\xi}\ . \tag{3.6}$$

In the following analysis, the study is confined to first- and second-order approximations in a weakly nonlinear framework, since the inclusion of higher-order boundary effects would considerably increase the complexity of the analytical formulation. In addition, these approximations are sufficient to describe the key physical processes influencing wave velocities and attenuation mechanisms.

3.1. First-order approximation

The unknown variables are expanded as power series to facilitate the approximation

$$\begin{gathered}v=\varepsilon v_1+\varepsilon^2 v_2+\ldots,\quad u=\varepsilon u_1+\varepsilon^2 u_2+\ldots,\quad \sigma^{ef}=\sigma_0^{(ef)}+\varepsilon\sigma_1^{(ef)}+\varepsilon^2\sigma_2^{(ef)}\ldots,\\ p=p_0+\varepsilon p_1+\varepsilon^2 p_2\ldots,\quad \phi=\phi_0+\varepsilon\phi_1+\varepsilon^2\phi_2\ldots,\quad e=e_0+\varepsilon e_1+\varepsilon^2 e_2\ldots,\\ V=V_0+\varepsilon V_1+\varepsilon^2 V_2\ldots,\quad R=R_0(1+\varepsilon R_1+\varepsilon^2 R_2\ldots).\end{gathered} \tag{3.7}$$

Here, we assume that $\beta=\alpha+1,\ \alpha=1$ and using formula (3.7), we collect the linear terms $\sim\varepsilon$ in the system (3.4):

$$\begin{gathered}\left(1-\phi_0\right)\rho_0^{(s)}c\frac{\partial v_1}{\partial\xi}+\frac{\partial\sigma_1^{(ef)}}{\partial\xi}-\left(1-\phi_0\right)\frac{\partial p_1}{\partial\xi}=0,\qquad \phi_0\rho_0^{(f)}c\frac{\partial u_1}{\partial\xi}-\phi_0\frac{\partial p_1}{\partial\xi}=0,\\ \rho_0^{(s)}c\frac{\partial\phi_1}{\partial\xi}-\left(1-\phi_0\right)c\frac{\partial\rho_1^{(s)}}{\partial\xi}+\left(1-\phi_0\right)\rho_0^{(s)}\frac{\partial v_1}{\partial\xi}=0,\\ -\phi_0 c\frac{\partial\rho_1^{(f)}}{\partial\xi}-\rho_0^{(f)}c\frac{\partial\phi_1}{\partial\xi}+\phi_0\rho_0^{(f)}\frac{\partial u_1}{\partial\xi}=0.\end{gathered} \tag{3.8}$$

The system (3.8) gives the integrals:

$$\begin{gathered}\left(1-\phi_0\right)\rho_0^{(s)}cv_1+\sigma_1^{(ef)}-\left(1-\phi_0\right)p_1=0,\quad \phi_0\rho_0^{(f)}cu_1-\phi_0 p_1=0,\\ \left(1-\phi_0\right)\rho_0^{(s)}v_1-\left(\left(1-\phi_0\right)\rho_1^{(s)}-\rho_0^{(s)}\phi_1\right)c=0,\quad \phi_0\rho_0^{(f)}u_1-\left(\rho_0^{(f)}\phi_1+\phi_0\rho_1^{(f)}\right)c=0.\end{gathered} \tag{3.9}$$

According to Eqs (2.3) and (2.6), the terms $\sim\varepsilon$ in the density series are:

$$\rho_1^{(s)}=\rho_0^{(s)}\left(\beta^{(s)}p_1-\frac{\beta^{(s)}\sigma_1^{(ef)}}{\left(1-\phi_0\right)}\right),\quad \rho_1^{(f)}=\rho_0^{(L)}\left(\beta^{(L)}\ell_1 p_1-4\pi n_0\ell_2 R_0^3 R_1\right). \tag{3.10}$$

and also: $$\rho_0^{(f)} = \ell_1 \ell_2 \rho_0^{(L)} \ , \tag{3.11}$$

where: $$\ell_1 = 1 - \frac{4\pi}{3} R_0^3 n_0, \quad \ell_2 = 1 + \beta^{(L)} p \ .$$

Using Eq.(3.11) and because of the conditions $v_1 = u_1$, $\rho_0 = (1-\phi_0)\rho_0^{(s)} + \phi_0 \rho_0^{(L)}$, the first two of the momentum Eqs (3.9) yield the following:

$$\rho_0 c v_1 = -\sigma_1^{(ef)} + \kappa_1 p_1 \ , \tag{3.12}$$

where: $$\kappa_1 = (1-\phi_0) + \frac{\phi_0}{\ell_1 \ell_2} \ .$$

Here, the linear terms $\sim \varepsilon$ in relations (3.6) and (3.5) give:

$$\begin{gathered} \frac{\partial v_1}{\partial \xi} + c \frac{\partial e_1}{\partial \xi} = 0 \ , \\ \sigma_1^{(ef)} - E_2 e_1 - \beta^{(s)} k_b p_1 = 0 \ . \end{gathered} \tag{3.13}$$

The linear terms $\sim \varepsilon$ in the bubble Eq.(2.2) give:

$$-\frac{1}{\rho_0^{(L)} \ell_2} (p_0 \chi R_1 + p_1) = 0 \ . \tag{3.14}$$

Eqs (3.13)-(3.14) give:

$$e_1 = -\frac{v_1}{c}, \quad \sigma_1^{ef} = E_2 e_1 + \beta^{(s)} k_b p_1, \quad p_1 = -p_0 \chi R_1 \ . \tag{3.15}$$

In Eq.(3.15), we can rewrite the effective stress $\sigma_1^{(ef)}$ as follows:

$$\sigma_1^{(ef)} = -\left[\frac{E_2 v_1}{c} + p_0 \chi \beta^{(s)} k_b R_1 \right] . \tag{3.16}$$

Here, from Eq.(3.13) and using p_1 from Eq.(3.15), the effective stress can be obtained as:

$$\sigma_1^{(ef)} = -(\rho_0 c v_1 + \kappa_1) p_0 \chi R_1 \ . \tag{3.17}$$

The combination of Eqs (3.16)-(3.17) gives:

$$\left(E_2 - \rho_0 c^2 \right) v_1 - \left(\kappa_1 - k_b \beta^{(s)} \right) p_0 \chi R_1 c = 0 \ . \tag{3.18}$$

Inserting Eqs (3.10)-(3.11) into mass equations (the last two equations in (3.9)) give:

$$(1-\phi_0)v_1 = \left[(1-\phi_0)\beta^{(s)}p_1 - \beta^{(s)}\sigma_1^{(ef)} - \phi_1\right]c\ ,$$
$$\phi_0 u_1 = \left[\phi_1 + \frac{\phi_0\beta^{(L)}p_1}{\ell_2} - \frac{4\pi n_0\phi_0 R_0^3 R_1}{\ell_1}\right]c\ . \tag{3.19}$$

The combination of Eq.(3.19) results in:

$$(1-\phi_0)v_1 + \phi_0 u_1 = \left[\frac{\left(\beta + (1-\phi_0)\beta^{(s)}\beta^{(L)}p_0\right)p_1}{\ell_2} - \beta^{(s)}\sigma_1^{(ef)} - \frac{4\pi n_0\phi_0 R_0^3 R_1}{\ell_1}\right]c\ . \tag{3.20}$$

Condition (3.1) means $v_1 = u_1$, therefore Eq.(3.20) becomes:

$$v_1 = \left[\frac{\left(\beta + (1-\phi_0)\beta^{(s)}\beta^{(L)}p_0\right)p_1}{\ell_2} - \beta^{(s)}\sigma_1^{(ef)} - \frac{4\pi n_0\phi_0 R_0^3 R_1}{\ell_1}\right]c\ . \tag{3.21}$$

Substituting Eq.(3.15) and p_1 from Eq.(3.14) into Eq.(3.21), we get:

$$\left(1-\beta^{(s)}E_2\right)v_1 + \left(\kappa_2 - k_b\beta^{(s)}\beta^{(s)}\right)p_0\chi R_1 c = 0\ , \tag{3.22}$$

where: $$\kappa_2 = \frac{\left(\beta + (1-\phi_0)\beta^{(s)}\beta^{(L)}p_0\right)}{\ell_2} + \frac{4\pi n_0\phi_0 R_0^3}{\ell_1 p_0\chi}\ .$$

Eqs (3.17) and (3.22) must coincide, therefore:

$$\begin{vmatrix} \left(E_2 - \rho_0 c^2\right) & -\left(\kappa_1 - k_b\beta^{(s)}\right)p_0\chi \\ \left(1-\beta^{(s)}E_2\right) & \left(\kappa_2 - k_b\beta^s\beta^s\right)p_0\chi \end{vmatrix} = 0\ . \tag{3.23}$$

Eq. (3.23) gives the velocity of the wave:

$$c^2 = \frac{\left(1-\beta^{(s)}E_2\right)A + E_2}{\rho_0}\ , \tag{3.24}$$

where: $$A = \frac{\left(\kappa_1 - k_b\beta^{(s)}\right)}{\kappa_2 - k_b\beta^{(s)}\beta^{(s)}}\ .$$

Thus, all the variables can express through the velocity v_1:

$$e_1 = -\frac{v_1}{c}, \quad \sigma_1^{(ef)} = -\left(E_2 - k_b \beta^{(s)} A\right)\frac{v_1}{c}, \quad p_1 = A\frac{v_1}{c}, \quad R_1 = -\frac{A}{p_0 \chi}\frac{v_1}{c},$$

$$\phi_1 = \left[\left((1-\phi_0) - k_b \beta^{(s)}\right)\beta^{(s)} A + \beta^{(s)} E_2 - (1-\phi_0)\right]\frac{v_1}{c}, \tag{3.25}$$

$$\rho_1^{(f)} = \rho_0^{(L)} A\left(\ell_1 \beta^{(L)} + \frac{4\pi n_0 \ell_2 R_0^3}{p_0 \chi}\right)\frac{v_1}{c}, \quad \rho_1^{(s)} = \rho_0^{(s)} \beta^{(s)}\left[A\left(1 - k_b \beta^{(s)}\right) + E_2\right]\frac{v_1}{c}.$$

Also, when $\beta^{(s)} k_b << 1$ and $\beta^{(s)} E_2 << 1$, the case of full-saturated soils (soft rocks) is considered. Accordinglly, Eqs (3.24)-(3.25) would be:

$$c^2 = \frac{(\kappa_1 / \kappa_2) + E_2}{\rho_0}, \tag{3.26}$$

$$e_1 = -\frac{v_1}{c}, \quad \sigma_1^{(ef)} = -E_2 \frac{v_1}{c}, \quad p_1 = (1/\kappa_2)\frac{v_1}{c}, \quad R_1 = -\frac{1}{p_0 \chi \kappa_2}\frac{v_1}{c},$$

$$\phi_1 = (1-\phi_0)\left(\frac{\beta^{(s)}}{\kappa_2} + 1\right)\frac{v_1}{c}, \quad \rho_1^{(f)} = \frac{\rho_0^{(L)}}{\kappa_2}\left(\ell_1 \beta^{(L)} + \frac{4\pi n_0 \ell_2 R_0^3}{p_0 \chi}\right)\frac{v_1}{c}, \tag{3.27}$$

$$\rho_1^{(s)} = \rho_0^{(s)} \beta^{(s)}\left(\frac{1}{\kappa_2} + E_2\right)\frac{v_1}{c}.$$

3.2. Second-order approximation

At the second order of smallness with respect to ε, combining the momentum Eq.(3.4) for the liquid and solid phases yields:

$$\rho_0 c \frac{\partial v_2}{\partial \xi} + \frac{\partial \sigma_2^{(ef)}}{\partial \xi} - \frac{\partial p_2}{\partial \xi} = \Sigma, \tag{3.28}$$

where: $$\Sigma = \rho_0 \frac{1}{2}\frac{\partial v_1}{\partial \tau}.$$

The linear terms of Σ are only considered. Here, collecting the quadratic terms $\sim \varepsilon^2$ in Eq.(3.5) gives:

$$\sigma_2^{(ef)} - E_2 e_2 - \beta^{(s)} k_b p_2 = T, \tag{3.29}$$

where: $$T \equiv \left[\sum_{q=1}^{6} a_q \, (-c)^q \, \varepsilon^{q-1} \frac{\partial^q e_1}{\partial \xi^q} - \sum_{q=1}^{4} b_q \left(-c\right)^q \varepsilon^{q-1} \frac{\partial^q \sigma_1^{(ef)}}{\partial \xi^q} \right].$$

Here, higher-order terms in ε are retained to account for small corrections to the leading-order behavior, as was done by Nikolaevskiy in [34]. These corrections ultimately manifest as perturbative modifications to the derived Nikolaevskiy equation later in this study, and they constitute the primary focus of the present research. Therefore:

$$\frac{\partial \sigma_2^{(ef)}}{\partial \xi} - E_2 \frac{\partial e_2}{\partial \xi} - \beta^{(s)} k_b \frac{\partial p_2}{\partial \xi} = \frac{\partial T}{\partial \xi} . \tag{3.30}$$

From Eq.(3.6) in the order $\sim \varepsilon^2$ we get:

$$\frac{\partial}{\partial \xi}\left(c e_2 + v_2 \right) = F, \quad F = -\frac{1}{c}\left(\frac{1}{2} \frac{\partial v_1}{\partial \tau} + \frac{\partial v_1 v_1}{\partial \xi} \right). \tag{3.31}$$

Therefore:

$$\frac{\partial e_2}{\partial \xi} = \frac{F}{c} - \frac{1}{c} \frac{\partial v_2}{\partial \xi} . \tag{3.32}$$

Substituting Eq.(3.32) into Eq.(3.30), we find:

$$\frac{\partial}{\partial \xi}\left(c\sigma_2^{(ef)} + E_2 v_2 - c\beta^{(s)} k_b \, p_2 \right) = E_2 F + c\frac{\partial T}{\partial \xi} . \tag{3.33}$$

Eqs (3.33) and (3.28) provide:

$$\frac{\partial}{\partial \xi}\left[\left(E_2 - \rho_0 c^2 \right) v_2 + \left(1 - \beta^{(s)} k_b \right) c \, p_2 \right] = E_2 F - c\Sigma + c\frac{\partial T}{\partial \xi} . \tag{3.34}$$

From the bubble Eq.(2.2), in the order $\sim \varepsilon^2$:

$$\frac{-\mu c}{\rho_0^{(L)} \ell_2}\left(4 + \frac{\phi_0 R_0^2}{k} \right) \frac{\partial R_1}{\partial \xi} = \frac{1}{\rho_0^{(L)} \ell_2}\left[\frac{\beta^{(L)} p_0 \chi}{\ell_2} p_1 R_1 + \frac{\beta^{(L)}}{\ell_2} p_1^2 + \frac{p_0 \chi (\chi + 1)}{2} R_1^2 - p_0 \chi R_2 - p_2 \right]. \tag{3.35}$$

Equation (3.35) can be rewritten:

$$p_2 = \Gamma - p_0 \chi R_2 , \tag{3.36}$$

where: $$\Gamma = \mu c\left(4 + \frac{\phi_0 R_0^2}{k} \right) \frac{\partial R_1}{\partial \xi} + \frac{\beta^{(L)} p_1}{\ell_2}\left(p_0 \chi R_1 + p_1 \right) + \frac{p_0 \chi (\chi + 1)}{2} R_1^2 .$$

Here, the substitution of p_2 from Eq.(3.36) in Eq.(3.34) gives:

$$\frac{\partial}{\partial\xi}\left[\left(E_2-\rho_0 c^2\right)v_2-\left(1-\beta^{(s)}k_b\right)p_0\chi R_2 c\right]=E_2F-c\Sigma+c\frac{\partial T}{\partial\xi}-c\left(1-\beta^{(s)}k_b\right)\frac{\partial\Gamma}{\partial\xi}\ . \tag{3.37}$$

For the sold and liquid-gas mixture, at second order, the combination of the linear terms from the mass balance equations Eq.(3.4) yields:

$$\begin{aligned}&\frac{\partial}{\partial\xi}\left[v_2-\left(\frac{\left(\beta+(1-\phi_0)\beta^{(s)}\beta^{(L)}p_0\right)p_2}{\ell_2}-\beta^{(s)}\sigma_2^{(ef)}-\frac{4\pi\phi_0 n_0 R_0^3\left(R_2+R_1^2\right)}{\ell_1}+\right.\right.\\&\left.\left.+\frac{4\pi\phi_0 n_0 R_0^3 p_0\chi\beta^{(L)}R_1^2}{\ell_1\ell_2}\right)c\right]=\Lambda\ ,\end{aligned} \tag{3.38}$$

where: $\Lambda=\dfrac{1}{2}\dfrac{\partial}{\partial\tau}\left[\left(\phi_1-(1-\phi_0)\beta^{(s)}p_1+\beta^{(s)}\sigma_1^{(ef)}\right)-\left(\ell_1\left(\phi_1\ell_2+\phi_0\beta^{(L)}p_1\right)-4\pi n_0\ell_2 R_0^3 R_1\right)\right]$.

From Eq.(3.33) we have

$$\frac{\partial\sigma_2^{(ef)}}{\partial\xi}=\frac{\partial}{\partial\xi}\left(T+k_b\beta^{(s)}\Gamma-k_b\beta^{(s)}p_0\chi R_2-\frac{E_2}{c}v_2\right)+\frac{1}{c}E_2F\ . \tag{3.39}$$

If we insert Eq.(3.39) and p_2 in Eq.(3.36) into Eq.(3.38), we get:

$$\begin{aligned}&\frac{\partial}{\partial\xi}\left[\left(1-E_2\beta^{(s)}\right)v_2-\left(Z_1p_0\chi-\frac{4\pi\phi_0 n_0 R_0^3}{\ell_1}\right)R_2 c\right]=\\&=\Lambda-\beta^{(s)}E_2F-c\beta^{(s)}\frac{\partial T}{\partial\xi}-cZ_1\frac{\partial\Gamma}{\partial\xi}+cZ_2\frac{\partial R_1^2}{\partial\xi},\end{aligned} \tag{3.40}$$

where: $Z_1=k_b\beta^{(s)}\beta^{(s)}+\dfrac{\left(\beta+(1-\phi_0)\beta^{(s)}\beta^{(L)}p_0\right)}{\ell_2}$, $Z_2=\dfrac{4\pi\phi_0 n_0R_0^3\beta^{(L)}p_0\chi}{\ell_1\ell_2}-\dfrac{4\pi\phi_0 n_0R_0^3}{\ell_1}$.

The determinant of the left-hand side of the system formed by Eq.(3.37) and Eq.(3.40) matches that of Eq.(3.23), which is equal to zero. A non-trivial solution for v_2 exists if the following compatibility condition is satisfied:

$$\begin{vmatrix} \left(E_2-\rho_0 c^2\right) & \dfrac{\partial}{\partial\xi}\left(E_2F-c\Sigma+c\dfrac{\partial T}{\partial\xi}-\left(1-\beta^{(s)}k_b\right)c\dfrac{\partial\Gamma}{\partial\xi}\right) \\ \left(1-E_2\beta^{(s)}\right) & \dfrac{\partial}{\partial\xi}\left[\Lambda-\beta^{(s)}E_2F-c\beta^{(s)}\dfrac{\partial T}{\partial\xi}-cZ_1\dfrac{\partial\Gamma}{\partial\xi}+cZ_2\dfrac{\partial R_1^2}{\partial\xi}\right] \end{vmatrix}=0\,. \tag{3.41}$$

This is the evolution equation with respect to $v \cong v_1$:

$$cN_1\frac{\partial\Gamma}{\partial\xi}-cN_2\frac{\partial T}{\partial\xi}+cN_3Z_2\frac{\partial R_1^2}{\partial\xi}+\Lambda N_3+c\Sigma\left(1-E_2\beta^{(s)}\right)-E_2FN_2=0\,, \tag{3.42}$$

where: $N_1=\left(1-\beta^{(s)}k_b\right)\left(1-E_2\beta^{(s)}\right)-Z_1N_3\,,\quad N_2=\left(1-\beta^{(s)}\rho_0 c^2\right),N_3=\left(E_2-\rho_0c^2\right).$

Now, we re-write Eq.(3.42) in terms of v and re-group:

$$\begin{gathered}\frac{1}{2}\left[Y_1+N_3\left((1-\ell_1\ell_2)\hat{\phi}_1-E_2\beta^{(s)}-\left(Y_2+\frac{4\pi n_0R_0^3}{p_0\chi}\right)A\right)\right]\frac{\partial v}{\partial\tau}+ \\ -\left[N_2c^2\left(a_1-b_1\left(E_2-k_b\beta^{(s)}A\right)\right)+\frac{N_1A\mu c^2}{p_0\chi}\left(4+\frac{\phi_0R_0^2}{k}\right)\right]\frac{\partial^2 v}{\partial\xi^2}+ \\ -\varepsilon N_2c^3\left[b_2\left(E_2-k_b\beta^{(s)}A\right)-a_2\right]\frac{\partial^3 v}{\partial\xi^3}-\varepsilon^2N_2c^4\left[a_3-b_3\left(E_2-k_b\beta^{(s)}A\right)\right]\frac{\partial^4 v}{\partial\xi^4}+ \\ -\varepsilon^3N_2c^5\left[b_4\left(E_2-k_b\beta^{(s)}A\right)-a_4\right]\frac{\partial^5 v}{\partial\xi^5}-\varepsilon^4N_2a_5c^6\frac{\partial^6 v}{\partial\xi^6}+\varepsilon^5N_2a_6c^7\frac{\partial^7 v}{\partial\xi^7}-G_N\frac{\partial vv}{\partial\xi}=0\,,\end{gathered} \tag{3.43}$$

where:

$$\hat{\phi}_1=\left((1-\phi_0)-k_b\beta^{(s)}\right)\beta^{(s)}A+\beta^{(s)}E_2-(1-\phi_0),\quad Y_1=\left(E_2N_2+c^2\rho_0\left(1-E_2\beta^{(s)}\right)\right),$$

$$Y_2=\phi_0\left(\ell_1\beta^{(L)}-\beta^{(s)}\right)+\beta^{(s)}\left(1-\beta^{(s)}k_b\right).$$

The nonlinearity coefficient is denoted by G_N, which is not present here since the further analysis of this study focuses on the linear part of Eq.(3.43).

We can write the short evolution equation Eq.(3.43) as follows:

$$G_1\frac{\partial v}{\partial\tau}-G_N\frac{\partial vv}{\partial\xi}=\sum_{q=2}^{7}\varepsilon^{q-2}G_q\frac{\partial^q v}{\partial\xi^q}\,, \tag{3.44}$$

where: $G_1=\dfrac{1}{2}\left[Y_1+N_3\left((1-\ell_1\ell_2)\phi_1-E_2\beta^{(s)}-\left(Y_2+\dfrac{4\pi n_0R_0^3}{p_0\chi}\right)A\right)\right],$

$$G_2 = \left[N_2 c^2 \left(a_1 - b_1 \left(E_2 - k_b \beta^{(s)} A \right) \right) + \frac{N_1 A \mu c^2}{p_0 \chi} \left(4 + \frac{\phi_0 R_0^2}{k} \right) \right],$$

$$G_3 = N_2 c^3 \left[b_2 \left(E_2 - k_b \beta^{(s)} A \right) - a_2 \right], \quad G_4 = N_2 c^4 \left(a_3 - b_3 \left(E_2 - k_b \beta^{(s)} A \right) \right),$$

$$G_5 = N_2 c^5 \left[b_4 \left(E_2 - k_b \beta^{(s)} A \right) - a_4 \right], \quad G_6 = N_2 a_5 c^6 \ , G_7 = -N_2 a_6 c^7 .$$

4. Results and discussion

The derived evolution equation is solved numerically to investigate the influence of gas bubbles on P1-wave propagation in porous media. The numerical simulations are performed using representative material parameters corresponding to water-saturated sandy sediments. The numerical values of the elastic moduli, viscosities, densities, and rheological parameters used in the simulations are summarized in Tab.1. These parameters are chosen based on typical values reported in the literature for fluid-saturated porous materials and bubbly liquids [23, 24, 35, 36].

According to the data of studies [30, 32, 37, 38], the parameter values for the rheological model presented in Fig.2 are:

The equilibrium bubble radius is taken as $R_0 = 5 \times 10^{(-4)}$:

$$M_1 = \rho^{(L)} L_s^2 = 10^{(-2)} kg/m, \quad M_2 = \rho^{(s)} L_s^2 = 0.02 kg/m, \quad M_3 = \rho^{(g)} L_s^2 = 2 \times 10^{(-6)} kg/m .$$

The corresponding elastic moduli are:

$$E_1 = 1/\beta^{(g)} = 4 \times 10^5 \, Pa, \quad E_2 = c^2 \rho_0 = 2 \times 10^7 \, Pa,$$

$$E_3 = 3 \chi p_0 = 4 \times 10^7 \, Pa, \quad E_4 = 1/\beta^{(L)} = 5 \times 10^8 \, Pa.$$

These values are calculated using a representative wave velocity of $c \sim 100 m/min$, and a characteristic oscillator length $L_s = 0.3cm$, as reported in [30, 39].

4.1. Influence of gas bubbles on wave velocity

To evaluate the influence of bubbles on wave propagation, we apply Eq.(3.24) to estimate wave speed. When bubbles are present, the wave velocity is approximately $484\ m/s$. In the absence of bubbles ($n_0 = 0$, $R_0 = 0$ and $M_3 = 0$), the velocity increases to around $656\ m/s$. This strong sensitivity arises from the high compressibility of the gas phase, which significantly alters the effective bulk modulus of the pore fluid.

This demonstrates that bubbles can significantly reduce wave speed, consistent with previous findings [25]. In the absence of gas bubbles, the predicted wave velocity is consistent with classical Biot-type results for fully saturated porous media. However, even a small concentration of gas bubbles leads to a pronounced reduction in wave velocity.

Further, applying Eq.(3.26) in the context of soft rock media yields a wave velocity of about $580\ m/s$ with bubbles, compared to approximately $776\ m/s$ without bubbles again assuming ($R_0 = 0$, $n_0 = 0$, and $M_3 = 0$).

Table 1. Setting of problem parameters.

Table 1 cont. Setting of problem parameters.

Parameter	Unit	Symbol	Value
Prosily	–	ϕ_0	0.38
Viscosity of gas	$Pa \cdot s$	μ_2	2×10^{-5}
Viscosity of water	$Pa \cdot s$	μ_1	10^{-3}
Permeability	m	k	1.8×10^{-11}
Bulk modulus	Pa	k_b	1.7×10^{9}
Steady pressure	Pa	p_0	10^{7}
Density of solid	kg / m^3	$\rho_0^{(s)}$	2500
Density of gas	kg / m^3	$\rho_0^{(g)}$	2
Density of water	kg / m^3	$\rho_0^{(L)}$	1000
Compressibility of solid	Pa^{-1}	$\beta^{(s)}$	2×10^{-10}
Compressibility of water	Pa^{-1}	$\beta^{(L)}$	2×10^{-9}
Compressibility of gas	Pa^{-1}	$\beta^{(g)}$	2.4×10^{-6}
Adiabatic exponent	–	ζ	1.4
Volume gas content	–	V_0	$10^{(-3)}$

4.2. Sensitivity analysis

Sensitivity analysis was carried out to assess the impact of key parameters on wave propagation characteristics. The analysis focused on the influence of bubble radius, bubble concentrations, and viscoelastic coefficients. The results show that an increase in equilibrium bubble radius causes a further decrease in wave velocity and an increase in attenuation due to enhanced bubble oscillations. Additionally, an increase in bubble concentrations causes an increase in dissipation effects, resulting in a decrease in phase velocity. However, an increase in viscoelastic stiffness parameters causes a partial compensation for bubble-induced softness effects, resulting in a moderate improvement in wave velocity. The results show that bubble-related parameters dominate wave behavior.

4.3. Comparison with existing models

In order to assess the performance of the developed three-branch viscoelastic model, a qualitative comparison is made with Biot's classical theory of poroelasticity and previously developed two-branch viscoelastic models. In Biot-type theories, the pore fluid is treated as a compressible constituent, without considering the dynamic effects related to the presence of gas bubbles. This leads to overestimation of wave velocities in partially saturated porous media, where bubble-induced oscillations play a crucial role.

In the context of Biot-type theories, the introduction of additional dissipation mechanisms, as described by the two-branch viscoelastic model, is more beneficial than the classical theory, as the former is capable of simulating certain attenuation mechanisms. However, these models lack the necessary flexibility to account for bubble-induced oscillations and their interaction with the solid skeleton, thus being less suitable for simulating wave propagation phenomena in partially saturated porous media. In the developed three-branch viscoelastic model, bubble-induced oscillations are incorporated as a separate constituent, thus providing a more detailed description of the related physical phenomena, with a more realistic reduction in wave velocity, as observed in porous media containing gas bubbles.

4.4. Computational aspects and practical relevance

From a computational point of view, the model under consideration results in a linear differential equation with constant coefficients, which can be solved using various numerical schemes. The extension of the model to include additional branches does not lead to numerical instability. Moreover, the linearization of the model eliminates the need for equation simplification and the use of iterative schemes. The model under consideration provides a theory for the interpretation of seismic and acoustic data in partially saturated media, such as reservoirs, marine sediments, and artificial porous materials, which can lead to applications in the fields of subsurface gas exploration and the study of the acoustic properties of porous composite materials.

5. Conclusions

A novel three-branch viscoelastic model has been proposed to simulate wave propagation in porous media with gas bubbles. The influence of gas bubbles has been specifically taken into account in the constitutive relations. The results show the strong influence of gas bubbles on the P1 wave velocities. Sensitivity analysis shows the dominance of the influence of gas bubbles compared to the influence of the viscoelastic properties of the solid matrix. The problem has been solved for one-dimensional wave propagation with weakly nonlinear conditions. The weakly nonlinear conditions are taken to preserve the analytical solution. The problem can be solved for multi-dimensional conditions with strong nonlinear conditions in the future. The theoretical predictions can be verified by experiments.

Nomenclature

k – permeability $\left[m^2\right]$
k_b – bulk modulus $\left[Pa\right]$
p – pressure $\left[Pa\right]$
R – bubble radius $[m]$
V_0 – volume gas content
$\beta^{(g)}$ – compressibility for gas $\left[Pa^{-1}\right]$
$\beta^{(L)}$ – compressibility for water $\left[Pa^{-1}\right]$
$\beta^{(s)}$ – compressibility for solid $\left[Pa^{-1}\right]$
μ – viscosity $\left[Pa \cdot s\right]$
ς – adiabatic exponent
$\rho^{(g)}$ – density for gas $\left[kg / m^3\right]$
$\rho^{(s)}$ – density for solid $\left[kg / m^3\right]$
$\sigma^{(ef)}$ – effective stress $\left[Pa\right]$
ϕ_0 – porosity

References

[1] Terzaghi K. von (1923): *Die Berechnung der Durchlässigkeit des Tones aus dem Verlauf der hydromechanischen Spannungserscheinungen*.– Sitzungsberichte der Akademie der Wissenschaften in Wien, Mathematisch-Naturwissenschaftliche Klasse, vol.132, pp.125-138.

[2] Terzaghi K. von (1925): *Erdbaumechanik auf Bodenphysikalischer Grundlage*.– Deuticke, Leipzig.

[3] Biot M.A. (1941): *General theory of three-dimensional consolidation*.– Journal of Applied Physics, vol.12, No.2, pp.155-164. https://doi.org/10.1063/1.1712892.

[4] Frenkel J.I. (1944): *To the theory of seismic and seismoelectric phenomena in saturated soil*.– Journal of Physics, vol.8, No.4, pp.230-241.

[5] Biot M.A. (1956): *Theory of propagation of elastic waves in a fluid-saturated porous solid. I. Low-frequency range*.– The Journal of the Acoustical Society of America, vol.28, No.2, pp.168-178. https://doi.org/10.1121/1.1908239

[6] Biot M.A. (1956): *Theory of propagation of elastic waves in a fluid-saturated porous solid. II. Higher frequency range*.– The Journal of the Acoustical Society of America, vol.28, No.2, pp.179-191, https://doi.org/10.1121/1.1908240.

[7] Biot M.A. (1962): *Mechanics of deformation and acoustic propagation in porous media*.– Journal of Applied Physics, vol.33, No.4, pp.1482-1498, https://doi.org/10.1063/1.1728759.

[8] Biot M.A. (1962): *Generalized theory of acoustic propagation in porous dissipative media*.– The Journal of the Acoustical Society of America, vol.34, No.9A, pp.1254-1264, https://doi.org/10.1121/1.1918315.

[9] Plona T.J. (1980): *Observation of a second bulk compressional wave in a porous medium at ultrasonic frequencies*.– Applied Physics Letters, vol.36, No.4, pp.259-261, https://doi.org/10.1063/1.91445.

[10] Nagy P.B. and Adler L. and Bonner B.P. (1990): *Slow wave propagation in air-filled porous materials and natural rocks*.– Applied Physics Letters, vol.56, No.25, pp.2504-2506, https://doi.org/10.1063/1.102872.

[11] Kelder O. and Smeulders D.M.J. (1997): *Observation of the Biot slow wave in water-saturated Nivelsteiner Sandstone*.– Geophysics, vol.62, No.6, pp.1794-1796.

[12] Smeulders D.M. (2005): *Experimental evidence for slow compressional waves*.– Journal of Engineering Mechanics, vol.131, No.9, pp.908-917. https://doi.org/10.1061/(ASCE)0733-9399(2005)131:9(908)

[13] Marin M. (1998): *Contributions on uniqueness in thermoelastodynamics on bodies with voids*.– Spanish Journal of Physics / Revista Española de Física, vol.16, No.2, pp.101-109.

[14] Marin M. (1997): *On the domain of influence in thermoelasticity of bodies with voids*.– Archives of Mechanics, vol.33, No.3, pp.301-308.

[15] Yadav A.K. (2023): *Magneto-thermo-piezo-elastic wave in an initially stressed rotating monoclinic crystal in a two-temperature theory*.– International Journal of Applied Mechanics and Engineering, vol.28, No.3, pp.124-142. https://doi.org/10.59441/ijame/172902

[16] Singh B. and Yadav A.K. and Gupta D. (2019): *Reflection of plane waves from a micropolar thermoelastic solid half-space with impedance boundary conditions*.– Journal of Solid Mechanics, vol.4, No.2, pp.122-131, https://doi.org/10.1016/j.joes.2019.02.003.

[17] Lotfy K., Elshazly I.S., Halouani B. Yadav A.K. and Elidy E.S. (2025): *Wave propagation in nonlocal piezo-photo-hygrothermoelastic semiconductors subjected to heat and moisture flux*.– Open Physics, vol.23, No.1, https://doi.org/10.1515/phys-2025-0162.

[18] Yadav A.K., Mahato H.S., Kumari S. and Jurczak P. (2024): *Analysis of reflection of wave propagation in magneto-thermoelastic nonlocal micropolar orthotropic medium at impedance boundary*.– International Journal of Numerical Methods for Heat & Fluid Flow, vol.34, No.9, pp.3416-3437, https://doi.org/10.1108/HFF-02-2024-0095

[19] Wijngaarden L. van (1968): *On the equations of motion for mixtures of liquid and gas bubbles*.– Journal of Fluid Mechanics, vol.33, No.3, pp.465-474, https://doi.org/10.1017/S002211206800145X.

[20] Wijngaarden L. van (1972): *One-dimensional flow of liquids containing small gas bubbles*.– Annual Review of Fluid Mechanics, vol.4, No.1, pp.369-396, https://doi.org/10.1146/annurev.fl.04.010172.002101.

[21] Tamura S. and Kawamura Y. and Tanaka H. (2002): *Effects of air bubbles on B-value and P-wave velocity of a partly saturated sand*.– Soils and Foundations, vol.42, No.1, pp.121-129, https://doi.org/10.3208/sandf.42.1121.

[22] Dunin S.Z. and Nikolaevskiy V.N. (2005): *Nonlinear waves in porous media saturated with live oil*.– Izvestiya, Physics of the Solid Earth, vol.51, No.1, pp.61-66.

[23] Dunin S.Z. and Mikhailov D.N. and Nikolaevskiy V.N. (2006): *Longitudinal waves in partially saturated porous media:*

The effect of gas bubbles.– Journal of Applied Mathematics and Technical Physics, vol.70, No.2, pp.251-263.

[24] Mikhailov D.N. (2010): *Influence of gas saturation and pore pressure on the characteristics of the Frenkel-Biot P-waves in partially saturated porous media*.– Izvestiya, Physics of the Solid Earth, vol.46, No.10, pp.897- 909.

[25] Dreyer W. and Duderstadt F. and Hantke M. (2012): *Bubbles in liquids with phase transition*.– Continuum Mechanics and Thermodynamics, vol.24, No.4-6, pp.461-483.

[26] Levitsky S. and Bergman R. and Haddad J. (2012): *Effect of size-distributed bubbles on acoustic properties of an elastic tube with polymeric liquid*.– International Journal of Multiphase Flow, vol.8, No.4, pp.469-488.

[27] Kudryashov N.A. and Sinelshchikov D.I. (2014): *Extended models of nonlinear waves in liquid with gas bubbles*.– International Journal of Non-Linear Mechanics, vol.63, pp.31-38, https://doi.org/10.1016/j.ijnonlinmec.2014.03.011.

[28] Dogan H. and White P.R. and Leighton T.G. (2017): *Acoustic wave propagation in gassy porous marine sediments: The rheological and elastic effects*.– The Journal of the Acoustical Society of America, vol.141, No.3, pp.2277-2288, https://doi.org/10.1121/1.4978926.

[29] Nikolaevskiy V.N. (1989): *Dynamics of viscoelastic media with internal oscillations*.– Soviet Mining Science, vol.25, No.3, pp.210-221.

[30] Nikolaevskiy V.N. and Strunin D.V. (2012): *The role of natural gases in seismics of hydrocarbon reservoirs*.– Elastic Wave Effect on Fluid in Porous Media, Proceedings 2012, pp.25-29.

[31] Ali A.A. and Strunin D.V. (2018): *The effect of rheology with gas bubbles on linear elastic waves in fluid-saturated granular media*.– International Journal of Applied Mechanics and Engineering, vol.23, No.3. pp.575-594, DOI: 10.2478/ijame-2018-0031

[32] Nikolaevskiy V.N. (1985): *Viscoelasticity with internal oscillators as a possible model of seismoactive medium*.– Doklady Akademii Nauk SSSR, vol.283, No.6, pp.1321-1324.

[33] Nikolaevskiy V.N. (1990): *Mechanics of Porous and Fractured Media*.– World Scientific, Singapore.

[34] Nikolaevskiy V.N. (2008): *Nonlinear evolution of P-waves in viscous–elastic granular saturated media*.– Journal of Mechanics of Materials and Structures, vol.73, No.2, pp.125-140.

[35] Olowofela J.A. and Adegoke J.A. (2004): *Modelling effective rheologies for viscoelastic porous media with application to silt and medium and coarse sand*.– Journal of Geophysics and Engineering, vol.1, No.3, pp.240-248, https://doi.org/10.1088/1742-2132/1/3/010.

[36] Sutton G.P. and Biblarz O. (2016): *Rocket Propulsion Elements*.– Wiley, New York.

[37] Nikolaevskiy V.N. (2016): *A real P-wave and its dependence on the presence of gas*.– Izvestiya, Physics of the Solid Earth, vol.52, No.1, pp.1-13.

[38] Nikolaevskiy V.N. and Stepanova G.S. (2005): *Nonlinear seismics and acoustic action on oil recovery from an oil pool*.– Journal of Petroleum Science and Engineering, vol.51, No.1, pp.131-139.

[39] Vilchinska N. and Nikolaevskiy V.N. and Lisin V. (1987): *Slow waves and natural oscillations in sandy marine soils*.– Izvestiya Acad. Nauk SSSR, Oceanology 4.

Received: September 14, 2025

Revised: March 30, 2026